Vulnerability of Axially Loaded Columns Subjected to Transverse Impact Loads

Thilakarathna H.M.I.[1], Thambiratnam D.P[2]., Dhanasekar M[3]., Perera N.J[4].

Abstract: Increased industrialisation has brought to the forefront the susceptibility of concrete columns in both buildings and bridges to vehicle impacts. Accurate vulnerability assessments are crucial in the design process due to possible catastrophic nature of the failures that can cause. This paper reports on research undertaken to investigate the impact capacity of the columns of low to medium raised building designed according to the Australian standards. Numerical simulation techniques were used in the process and validation was done by using experimental results published in the literature.

The investigation thus far has confirmed that vulnerability of typical columns in five story buildings located in urban areas to medium velocity car impacts and hence these columns need to be re-designed (if possible) or retrofitted. In addition, accuracy of the simplified method presented in EN 1991 to quantify the impact damage was scrutinised. A simplified concept to assess the damage due to all collisions modes was introduced. The research information will be extended to generate a common data base to assess the vulnerability of columns in urban areas against new generation of vehicles.

Keywords: Dynamic analysis, Numerical simulations, Lateral impact, Structural columns

1. Introduction

Exposed column in underground car parks and the columns of medium to low rise buildings located near the roads are highly vulnerable to impact loads due to moving vehicles. For instance, around 35% of the vehicle crashes involves building columns, traffic lights and light poles and cost Australian society around $ 4.6 billion per year [1]. Catastrophic failure of supporting bridge and building as a result of the impact worsen the consequences and may require proper analysis techniques which can be used for routine column design as well as damage mitigation.

Impact capacity of medium to low raised building columns made out of Grade 47 concrete are investigated in this paper by using explicit numerical simulation procedure which can simulate transient analysis problems. This procedure can also account for the dynamic behaviour of the impacted column, plastic deformation of the impacted vehicle, additional stiffness provided by the axial load on columns as well as the confinement effects and strain rate effects. In addition, possible collapse due to higher mode of vibrations, combine flexure and shear failures due to typical low elevation impact are also taken in to account.

An impact pulse generated from a typical car to rigid barrier impact was used to reconstruct the vehicle impact. This method will eliminate the uncertainty of the stiffness and the residual velocity component from the analysis process. The attractiveness is that it can be used as a foundation to generate a data base which can be used to determine the vulnerability of column against the impact of new generation of vehicle under all modes of collisions.

2. Validation of the of the Finite Element Model

2.1. Experimental setup and material properties of the tested columns

Experimental results of the Feyarabend [2] column tests were used in the validation process. The column was tested in a horizontal position as shown in Figure 1. Fixed support conditions were achieved by stationary steel sections fixed at the ground and the

[1] PhD Student, School of Urban Development, Queensland University of Technology
[2] Professor, School of Urban Development, Queensland University of Technology
[3] Professor, School of Urban Development, Queensland University of Technology
[4] Adjunct Professor-QUT, Robert Bird Groups

other end was hinged and free to slide parallel to the longitudinal axis of the column while being restrained by a 20t mass. The mass can slide over horizontal low friction rails. The axial load is applied by using restressing wires located either sides of the column and impact load was generated by dropping the 1.14t mass on to the column at mid span.

The testing procedure involved impact test on 300x300mm rectangular column specimens made out of Grade 47 concrete. Under the mid span impact the column has reached near failure conditions. The properties of the test specimen are tabulated in Table 1.

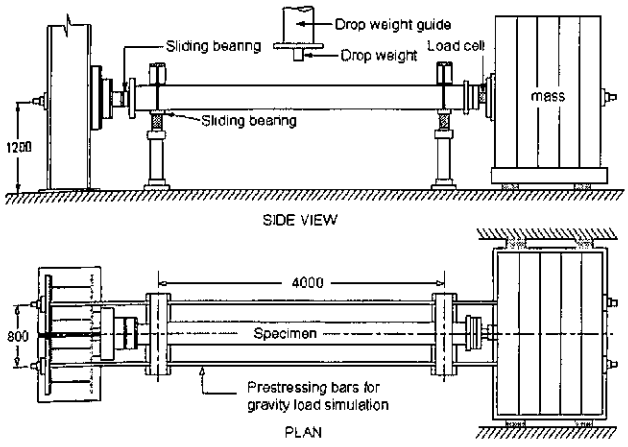

Figure 1: The test set-up by Feyerabend

Test	SB1
Cross-section (mm)	300x300
Span (m)	4.0
Cube strength, f_{cu} (MPa)	44
Yield stress, f_y (MPa)	482
Main bars, A_s	4ϕ18
Shear reinforcement, A_{sv}	12ϕ@150
Restraining mass (t)	20
Initial axial load (kN)	-245
Striker mass (t)	1.14
Impact velocity (m/s)	1.5/3.0
Velocity at which f_y was reached (m/s)	±1.5

Table 1: Characteristics of the Feyerabend's test specimens

2.2. Development of the Numerical model

As the entire structure does not have enough time to respond to a rapid change of loading under impact conditions [3], it is assumed that the lateral movements of the restraining mass and the elongation of the prestressing cable system during the impact do not affect the impact behaviour of the column. Hence, the prestressed cable was neglected and the axial load applied as a surface pressure over the cross section.

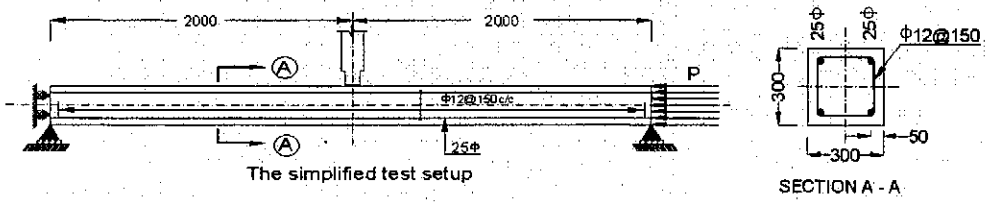

Figure 2: The simplified test set-up and the cross section

The simplified set-up of the impacted column is shown in Figure 2. The simulation was carried out with a half model and boundary conditions were introduced to ensure the symmetry conditions. The concrete beam was modelled using 25mm eight node hexagonal solid element with one point integration. In order to prevent contact break downs, similar mesh distritization was used for the drop weight at the contact interface [4]. Numerical convergence study shows that further decrease of the mesh size has only a very little effect on the accuracy of the results while increasing the duration of the analysis dramatically. Similarly, 25mm long beam element was used for both vertical and the lateral reinforcements with 2x2 Gauss integration. Moreover, the vertical reinforcements were defined as truss elements and the links were defined as a Hughes-Liu beam element with cross sectional integration [5]. Eight nodes hexagonal solid elements with one point integration were employed for the drop mass. Initial analysis was carried out by assigning rigid body conditions.

As far as deformed reinforcement bars are concerned, the ultimate bond at failure was 70-100% higher than that under quasi-static loading conditions [6]. Also, the steel deformation under the impact load was limited to a region only few centimetres long beneath the point of the impact [7]. This means that there was no enough time to develop extensive bond slip along the length of the bar under impact condition. Therefore, perfect bond is assumed between the reinforcement and concrete.

2.3. Material characteristics

Concrete columns are susceptible to brittle failures under impact loads. Several material models in LS-DYNA capacitate to simulate the brittle behaviour of impacted concrete. However, the nonlinear softening behaviour of concrete after yielding of reinforced concrete is not very well simulated by these models. In addition, some of these models include many parameters that can not be determined by general testing procedures. 'Concrete Brittle Damage Model' presented in LS-DYNA library is extremely useful in this circumstance as it employs a fully anisotropic damage rule which is free from adjustable parameters for a given failure surface [8].

It is well known that numerical results are very sensitive to the nonlinear material properties. In the absence of more specific data for the dynamic properties of concrete the following equation presented an approximate value for tensile limit of concrete [9].

$$T_{Limit} = 1.58\left(\frac{(f'_c)^2}{a_o}\right) \qquad 1$$

where compressive strength (f'_c) should be in MPa and a_o is 145 for SI units. Once the principle tensile stress has been reached at a point, a smeared crack is initiated at that point with a normal that is co-linear with the first principle direction. Allowed tensile traction normal to the crack plane is progressively degraded as the loading progresses. This behaviour is implemented by reducing the material modules normal to the smeared crack plane by using program based internal parameter. In addition, shear strength basically governs the initial shear traction that may be transmitted across a smeared crack plane. Govindjee, Key and Simo [8] presented a full description of the tensile and shear damage part of this material model.

In order to avoid error termination, values of viscosity (η) between 0.71 to 0.73MPa are recommended [4]. Apart from serving as regularizing parameter which stabilizes the calculations, the viscosity of the material also allows the inclusion of first order rate effects during the simulation. However, an inconsistency is found when quantifying of the fracture energy under high strain rate conditions. Also, no specific guidelines are found in the CEB-FIP model code [9] related to the strain rate effects on fracture toughness. Therefore, strain rate effects are exempted from the fracture toughness and a value selected based on the static material characteristics similar to the one that carried out by Unosson [5].

Instead of using stress-strain relationship, the impact behaviour of concrete was defined by using various parameters which simulate the non-liner behaviour of concrete. Table 2 shows the reasonable values selected for Grade 47 concrete. In the absence of the definite data modulus elasticity of concrete (E_{ci}) was calculated by using following equation [9];

$$E_{ci} = E_{co}\left[(f_{ck} + \Delta f)/f_{cmo}\right]^{1/3} \qquad 2$$

where f_{ck} is the characteristic cylindrical strength of concrete and Δf is equal to 8 MPa, f_{cmo} is 10 MPa and E_{co} is 2.15×10^4 MPa. The shear retention factor was selected by using trial and error method. The cylinder compressive yield strength (σ_y) should be used here and cylinder strength can be directly calculated from the uni-axial cubic strength by using the Table 2.1.1 of CEB-FIP code [9].

Table 2: Material properties used for the concrete

Density (kg/m^3)	E_{cl} (GPa	ρ	Tensile limit (MPa)	Shear limit (MPa)	G_c (Pa)	Shear retention	Viscosity η (Mpa)	σ_y (MPa)
2381	35.5	0.21	3.77	17.7	150	0.025	0.71	35.4

2.4. Material properties of steel

Longitudinal steel and links were modelled as an elastic perfectly-plastic material by using Mat_Plastic_Kinematic model which is know as a very cost effective as far as the duration of the analysis is concerned. In this simulation, Kinematic hardening was implemented including rate effects. *S* and *P* are the usual parameters of the Cowper Symonds equation. Table 3 represents the material properties adopted for main reinforcement in this simulation.

Table 3: Material properties used for the reinforcement

Density (kg/m^3)	E_s (GPa)	Poisson's ratio ρ	σ (MPa)	E_t (GPa)	Hardening Parameter (β)	S	p
7800	210	0.30	548	2.0	0	40	5

As the falling weight of 1.14t did not experience excessive deformations, rigid material model was implemented for the impacting mass. Rigid elements are bypassed in the element processing and no storage is allocated for storing history variables. However, the inertial properties of the materials are calculated from the geometry of the elements and hence the realistic values for the density and the modules of elasticity must be provided [4]. In addition, when the rigid body interact with the column, the sliding interface parameters are determined by using the given E and ρ values of the material [4]. The material characteristics used for the drop mass are given in Table 4. Abbreviations CON1 and CON2 are dealing with the displacement and rotational constraints of the rigid body about global X and Y directions.

Table 4: Material properties used for the Rigid Body

Density (kg/m^3)	Young's Modulus (GPa)	Poisson's ratio	CMO	CON 1	CON2
7800	210	0.3	1	4	7

2.5. Load simulation for the dynamic system

When imposing static loads in explicit environment the ramp up loading would be the better solution to avoid the stress fluctuation. The ramp up load must be increased from zero to its final value and the load curve should extend beyond the termination line for stability. In general, the ramping duration should be grater than the natural frequency of the column. Apart from that it is observed that the stabilisation depends on the wave speed and the superimposing effects of the reflected waves at the boundaries. The minimum fluctuation was observed when the ramping duration was around 0.02s, where as further increments disturbed the stabilisation. The lateral impact force must be applied only after the stabilisation. As the distance between the rigid body and the column remained constant (say 10mm), the 'Loading Curve' used for the rigid body must fulfil the conventional equations of motion.

2.6. Reduction of the hour glass energy

The under integrated elements are more robust in large deformation calculations because the strain terms evaluated at the integration point remain well conditioned at larger deformations. However the disadvantage is that some modes of deformation may caused hourglass problem and may leads to inaccurate results. In addition, it is interesting to note that the hourglass deformation modes are orthogonal to the strain calculations and hence work done by the hourglass resistance is neglected in the energy equation. The hourglass resisting force vectors are given by the following equation [4].

$$f_{i\alpha}^{\ k} = a_h h_{i\alpha} \Gamma_{\alpha k} \qquad 3$$

$$\text{where } a_h = Q_{hg} \rho \, v_e^{2/3} \frac{c}{4}. \qquad 4$$

In which v_e is the element volume, c is material sound speed, and Q_{hg} is a user defined constant and when Q_{hg} is equal to 0.05, improved results have been observed. As this equation contains a component of the volume v_e, theoretically the hourglass error should reach to zero with the mesh refinements. Moreover, the default setting of LS-DYNA which is given by the Equation (3) is not orthogonal. Hence, the orthogonal approach, as described by Flanagan and Belytschko [10] is implemented in this simulation. Hourglass energy can also be minimised in expense of solution time by decreasing the time step size which introduce slightly higher stiffness to the numerical model. However further effort has not been taken to converge the results as the hourglass energy become negligible with the implementation of the above procedures.

2.7. Numerical results

The comparison of the load-deflection curves of the numerical simulation and that of the experimental test are presented in Figure 3. The resultant maximum deflection and duration of the impact are well reflected by the numerical simulation. Therefore, the inertia stiffness of the impacting bodies, boundary conditions and effects of confinement are reasonably simulated by the numerical model. Also, it is important to note that the residual displacement of the column was reasonably approximated by the numerical results even after the cracking and slight crushing of the concrete occurred simultaneously during the impact. The amount of crushing is important as this can be decreased the amount of energy available to absorb as strain energy during an impact. Excessive amount of crushing will disturb the post impact behaviour of the column.

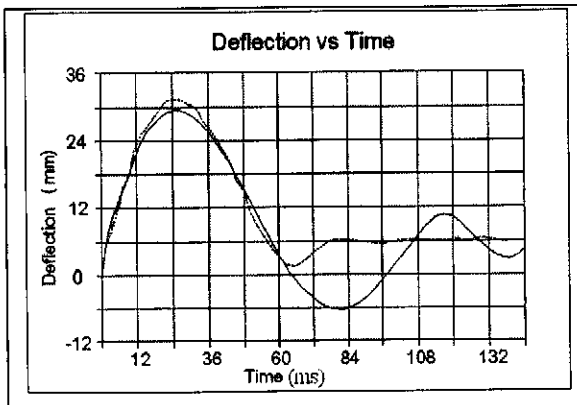

Figure: 3 Comparison of the resultant deflection

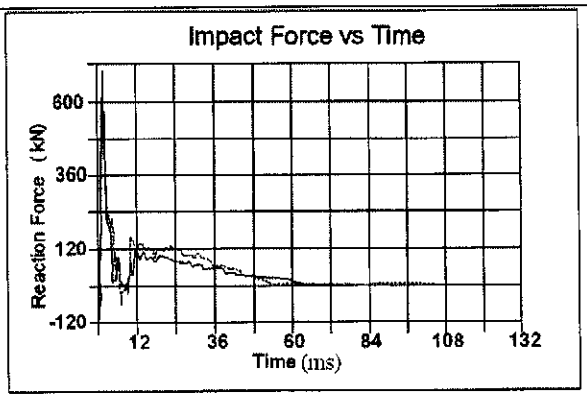

Figure: 4 Comparison of the resultant impact force

In Figure 4, the continuous line represents the contact force history obtained through the numerical simulation and the dotted line represents the one that obtained from the experimental test. It can be seen that the variations are almost identical and the

differences between those two graphs are within 10% range. On the other hand, exact simulation of the peak contact force is an evidence of the accurate representation of the stiffness and boundary conditions as it would mainly depend on the inertia characteristics of the column for given boundary conditions. However, significant differences are observed in reaction forces generated by the numerical simulation and the experimental results (Figure 5). One of the reasons behind this variation may be the filtering procedure used to extract the data from the data logger system [21].

The resultant crack propagation in the numerical simulation and experimental data are presented in Fig. 6. Tension cracks were initiated at the bottom and top of the beam followed by the crushing of the material beneath the impacted zone. The simulation reproduced the tension crack at the bottom while displaying dense tensile crack propagation at the top surface of the beam. The dense crack concentration occurred directly beneath the impacted zone with the partial separation of the material represented as a region with higher stress accumulation. Based on these factors, it can be concluded that the numerical simulation reasonably follow the impact behaviour of the axially loaded column.

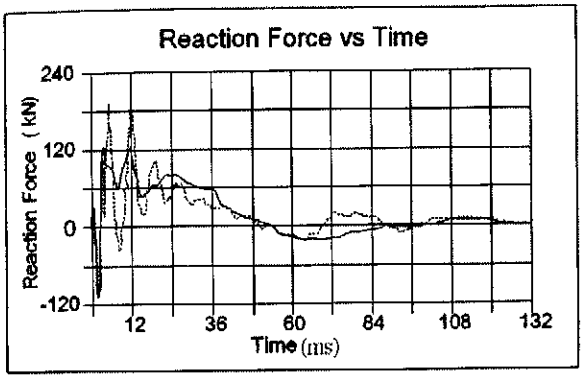

Figure: 5 Comparison of the resultant reaction force

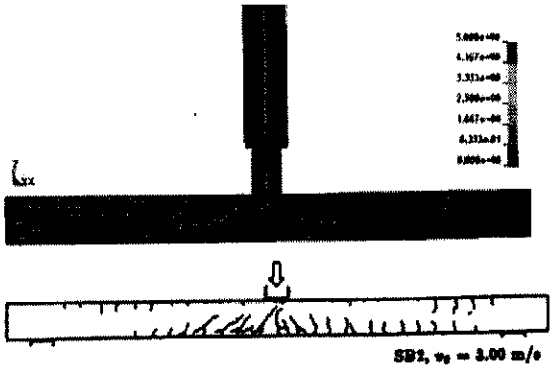

Figure 6: Crack Propagation of the impacted column and numerical simulation

3. Impact reconstruction using crash test data

It is complex to generate realistic numerical models of vehicles for impact reconstructions. On the other hand, the simplified methods that are used in the past limit their application to asses the vulnerability of columns against general vehicle population. The crash response depends on the mode of impact, rate sensitivity of the vehicle, dynamic crush, restitution, collision partner and vehicle specific parameters [11]. Therefore, the force time history of an impact at one particular velocity is different from vehicle to vehicle even thought the mass is the same. Consequently impact reconstruction with rigid body or even with the simplified deformable body assumption may not be very accurate. For instance, a typical contact force history obtained through the rigid body impact with a concrete column has two force pulses and the main pulse lasts only for about 5ms. Similarly maximum resulting dynamic interaction force calculation based on 'Hard Impact' assumption [12] is exceptionally sensitive to the equivalent elastic stiffness of the object (i.e. the ratio between force F and total deformation). Due to the inherent relationship between the force (amplitude) and the total deformation, the dynamic interaction force [12] is not inappropriate to represents the impact response of a vehicle population having a unique mass.

Table 5: Comparison of the rigid barrier impact data with properties of the Impulse

Vehicle	Velocity $V(ms^{-1})$	Mass M (kg)	Impact Duration (s)	(MV)	Area of the curve	% variation
Ford Explorer	16.9	2242	0.150	37890	39573	1.04
Ford Taurus	15.6	1619	0.100	25274	27794	1.09
Renault Fuego	13.3	1329	0.100	17793	16687	0.94

Table 5 compares the area of the triangular impulse generated from the full scale crash tests with the product of mass and the velocity of the respective vehicles [13]. The force time history was obtain by using the data generated by the accelerometer placed at the centre of gravity of the impacted vehicle. It is evident that the force pulse generated from the realistic impact events agree well with the product of mass and the velocity for range of impact scenarios. This will ensure the accuracy of the test data and eliminate the uncertainty of the amplitude from the Force-Time history diagram. This will also enable accurate prediction of the vulnerability of the column for the respective vehicle impact. In fact, force time history data generated from vehicle impact with rigid barriers are always conservative for the vulnerability assessment of the concrete columns. Therefore, in the absence of realistic numerical models of vehicles, the vehicle column interaction can be conservatively regenerated by using the force time history diagram resulting from the rigid barrier-vehicle impact events.

3.1. Impact pulse modelling and vulnerability prediction

Numerous models have been proposed to simulate the impact pulse with varying success. Sine, haversine, triangular and square formats are the standard formats that have been widely used to represent the frontal barrier impact [14]. To investigate the efficiency of the various curves to simulate the collision pulses, force histories generated from several full scale frontal collision scenarios were studied. The MATHLAB program can be used to generate the ideal curve by using accelerometer data alone and hence derivation of mathematical model for different curves by using parameters such as velocity profile, frontal stiffness, residual deformation and restitution is not considered at this stage. Based on this method several force time histories derived by using accelerometer data presented in SAE [13] are compared in the following paragraph.

Comparisons of the Force -Time history of the Honda Accord, Ford Taurus & Renault Fuego are shown in Figure 7. Durations of the impacts were 100ms and triangular pulse shape is best fitted with the force history diagrams. This pulse shape has already been identified as a useful collision pulse model to simulate the frontal impact conditions [14]. While the pulse shape best represented by the triangular model, the area under the extrapolated curve can be used to predict the force histories at various speeds. Alternatively, if the impact pulse which causes the instability of the column is known, the extrapolated pulses can be used to determine the velocity of the vehicle that caused the damage. However, as the duration of the impact is kept constant, this method is conservative only for vulnerability prediction at higher velocities.

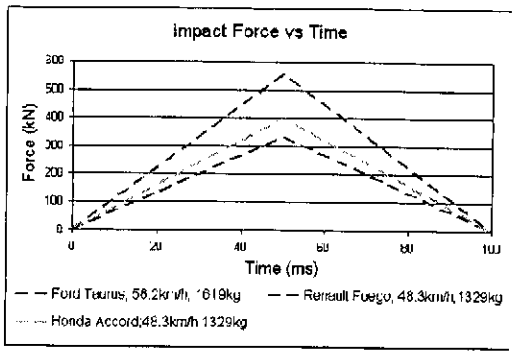

Figure 7: Force Time histories of full scale crash tests

4. Impact behaviour of axially loaded columns of medium rise buildings

Impact capacity of identical braced columns of five to twenty storied buildings made out of Grade 47 concrete was investigated by using comprehensive numerical simulations. Considered columns are supporting 5.5m spaning slabs in each direction which carries 3kN/m^2 live load identical to the design load capacity of an office building, classrooms or lecture theatres at each floor level [15]. It is assumed that the access road is provided through the ground floor level and vulnerability of the columns were assessed for a frontal collision of light weight vehicles such as cars or vans. The structural design was carryout by assuming general design prospective according to AS3600 standards [16]. Therefore, priority was given to the constructability, common section sizes and the availability of the materials such as reinforcement steel rather than perform an analysis which considers the overall aspects of a research in terms of parametric studies. However, for comparison purposes the axial stresses on the columns is maintained approximately constant rather than the axial load on the columns. This leads to smooth graphs at the later stage and basically two alternative design options were considered in the first phase. The first option was based on the maximum steel ratio while the second option based on the minimum steel ratio. Figure 8 represents the cross sections of the selected columns for different storey height.

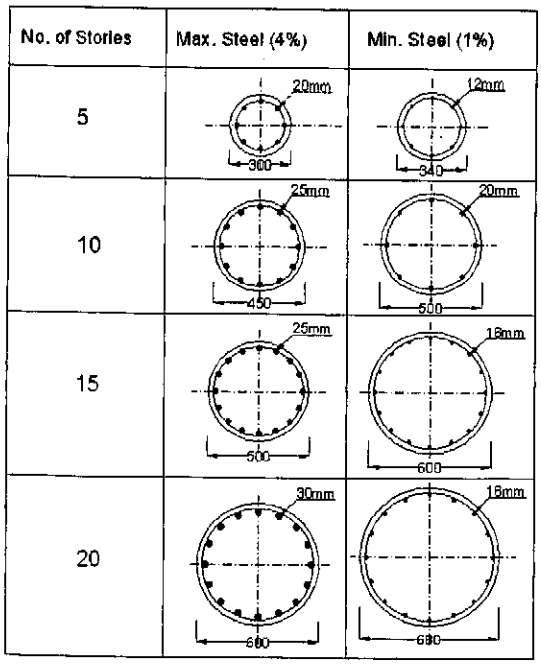

Figure 8: Cross sectional area of the circular concrete columns

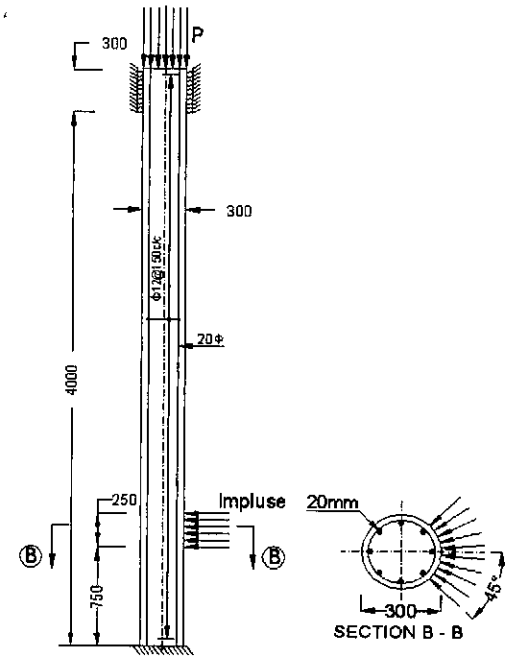

Figure 9: Support conditions and external loads applications

Fixed support conditions were assumed in this analysis. Translations as well as the rotations of all the nodal point in all directions are restrained at the bottom. In order to achieve the fixed end condition at the top, the lateral movements of the circumferential nodal point were restrained in the global X and Y directions (Figure 9). The restrained height is maintained equal to the diameter of the column to achieve the fixed end conditions [17]. The free movement of the column along the Z direction was allowed in order to permits axial shortening under the axial load application as well as allow free vertical movements of the column during an impact. On the other hand, by adjusting the restraint height, this support condition can be extended to simulate a support condition which will provide only a nominal restraint. This will allow the comparison of the impact behaviour of columns under different support conditions.

4.1. Numerical simulation of the impacted columns

Finite element mesh generation for concrete column can be done by using either cube or wedge elements. The mesh generation associated with the wedge elements is moderately large and multiple elements have to share one single node at the centre. This causes stability problems if the element undergoes severe deformations [6]. As the implemented failure criterion is based on the residual capacity of the column large deformations are unavoidable. To avoid element inter locking Cartesian coordinate system was used at the centre similar to the one shown in Figure 10. Obviously, the number of elements generated inside the rectangular section is quite large and hence, stability of this model is high when it undergoes large deformations. However, this method creates a large number of small elements in the model having small cross sections. These cubic elements are the smallest elements in the entire model and the time step size is governed by the size of these elements.

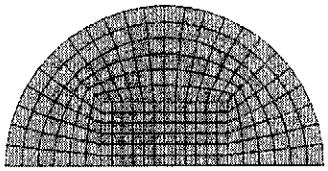

Figure 10: Plan view of the half models

The vertical reinforcements were modelled with truss elements and links with beam elements similar to the validation process. By implementing 1D elements modelling effort as well as the duration of analysis can be minimised. Grade 47 concrete and the previously defined steel properties were used here and hence will not be addressed again. As far as the strain rate effects are concerned, they are not so predominant because of the shear type of failures of the columns with low amount of deflection. On the other hand, it is revealed that the effect of the impact is localised and the average stain rate is well below $0.1s^{-1}$ even under high velocity impact conditions [18-21]. However the first order rate effects are already included in the validation process and that can be minimised the deviation due to the higher order variation. In fact, parameter sensitivity under low velocity impact conditions mainly occurred as a result of strain rate effects and the second order rate effects mainly occurred due to the inertia effects of the impacted column. Therefore, error introduce in to the model due to the rate sensitivity of the material will be minimised.

4.2. Axial and lateral load applications

Axial load on the column can be applied as a uniform pressure over the concrete area or as combination of loads on the steel and concrete areas separately by assuming uniform strain distribution. Researchers used the first option based on the assumption that perfect bond between the concrete and steel can generate the uniform strain condition. However it would be worth to investigate the above options in detail and select the one that minimise the error due to the contact enforcement.

In order to achieve the uniform strain condition a column subjected to pure axial compression must fulfil the following requirement.

$$\varepsilon_c = \varepsilon_s \qquad 5$$

where ε_c and the ε_s are represent the longitudinal strain in concrete and steel respectively. For linear elastic behaviour, stresses in concrete and steel are in proportion to the modular ratio, $n = E_s / E_c$. Then by considering axial load compatibility, it is possible to derive the following equation.

$$\sigma_c = \frac{N}{A_c} \frac{1}{1 + n\rho_{total}} \qquad 6$$

where N is the axial load on the column and A_c is the cross sectional area of the concrete column. ρ_{total} is the steel ratio of the section. This equation is based on the assumption that strain of concrete and steel vary in identical manner under the axial loads which is not particularly true at the ultimate stage. However the usual case is the longitudinal steel yield prior to the concrete and with the implementation of the axial load reduction factor ϕ according to AS 3600 [16], the error induced by the previous procedure can be neglected.

Deflection of the column under the separate application of axial load on steel and concrete areas was different from the one with uniformly distributed load. This will cause a substantial difference of the failure load at near ultimate stage. That means the fully bond between concrete and steel will not ensure the equivalent strain distribution. The resultant stress concentration at the top of the column with the application of the uniform pressure caused the deviation. On the other hand, wave propagation effects through the material may alter due to the stress concentration. It is also observed that the separate application of axial load perform well as far as hourglass is concerned. This means the uniform pressure distribution on the column may leads to unrealistic behaviour of the impacted column at a later stage. This will introduce an error to the outcomes and hence the numerical simulation process must contain a contact enforcement verification phase other than the consideration of the mesh discritization.

As far as lateral load applications are concerned, the collision force F may be applied at impact height of 0.50m above the level of the carriageway particularly for a car impact [12]. The recommended application area is 0.25m high and must be applied across the entire width of a column. By assuming that the rigid foundations of the buildings are located 0.375m beneath the ground level, the impact height was taken as 0.750m above the level of fixity of the column as shown in Figure 9.

4.2.1. Impact capacities of identical building columns

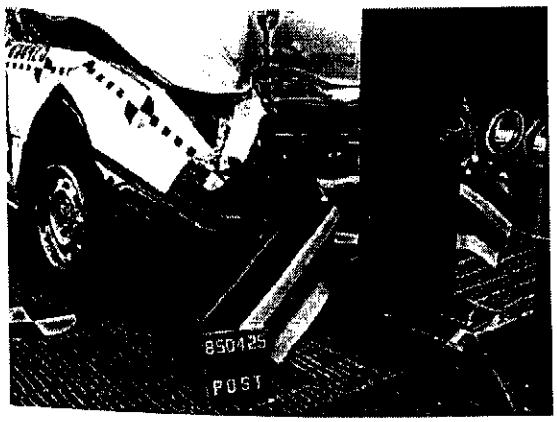

Figure 11: Honda Accord in a frontal collision at a speed of 48.3km/h (SAE)

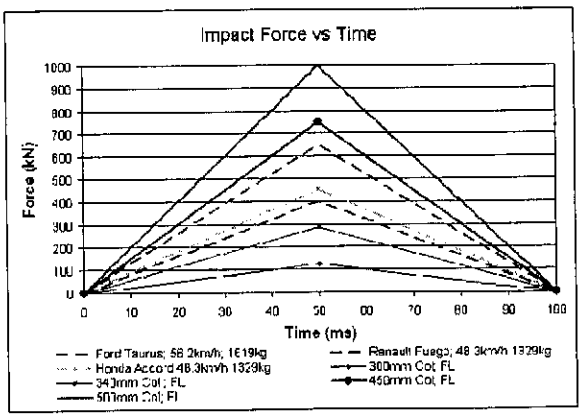

Figure 12: Comparison of impact capacities of fully loaded (FL) columns with full scale crash tests

300mm column and 340mm column are the typical axially loaded columns of five-storey buildings with the two different (1% & 4%) steel ratios respectively (See Figure 12). Based on the correlation that the area under the force history curve represents the product of mass and the velocity of the impacting vehicle, it can be calculated that the axially loaded five-storey building column can survive from the car impact only if the impact velocity is less than about 15km/hr or 40km/hr. This velocity is within the range of velocities that can be achieved in an urban area and hence fully axially loaded column having diameters equal to or less than 340mm are likely to collapse under medium velocity car impact. On the other hand, 15km/hr is a typical velocity condition that can be achieved even in a courtyard [16]. These statements can not be generalised due to the different frontal stiffness of the vehicles. However by representing the impact capacity of the columns in terms of force history diagram, it may be able to predict the vulnerability of the impacted columns against new generation of vehicles once the impact force generated by a frontal or oblique collision has quantified. By this means, force history diagrams will generate a common platform to assess the vulnerability of the columns for any kind of vehicle impact.

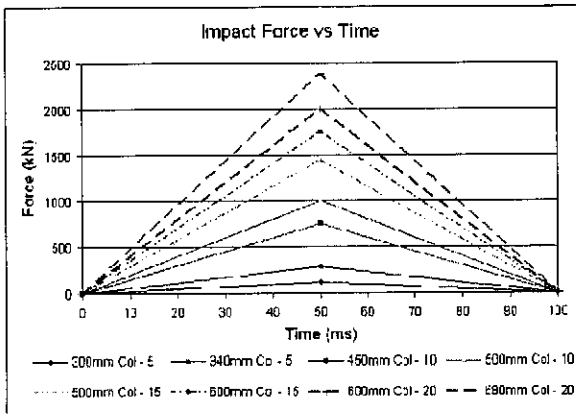

Figure 13: Ultimate capacities of impacted columns

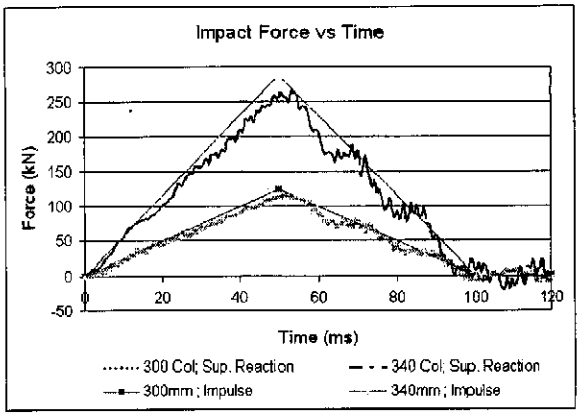

Figure 14: Support reaction and the Impact pulse

Comparison of the maximum impact capacities of impacted columns up to twenty-storey buildings in terms of Force-Time history is given in Figure 13. According to the Figure 12, the maximum impact force applied by medium velocity car impact is around 650kN. Therefore it is evident that axially loaded columns in ten-storey and above will not be susceptible to collapse under medium velocity car impact.

Figure 14 represents the support reaction and the applied lateral impact pulse on the column during an impact simulation. The reaction forces are nearly equal to the applied impact pulse as inertia effects and damping effects are less pronounced under shear failure conditions. By definition, for 'hard impact' it is assumed that the structure is rigid and immovable and that the colliding object deformed linearly during the impact phase [16]. Based on that assumption an equation was derived in EN 1991 [16] to calculate the maximum resulting dynamic interaction force applied on the impacted column. However, the aforementioned difference actually represents the probable error that might occur in interaction force determination based on the undeformable impacted body assumption. Therefore, this assumption may only be true for the shear failure predominant columns. Consequently, the analysis based on this assumption may need amplification factor which can account for the inertia and damping effects under flexural failure predominant column. Therefore, undeformable body assumption used in EN 1991 is conservative for flexural failures predominant columns.

5. Conclusions

- According to the El-Tawil [3], connecting structures does not have enough time to contribute to the dynamic behaviour of the impacted column under impulsive loading conditions. This observation is effective in simplifying the numerical models of impact simulations.

- Assumption of perfect bond between steel and concrete is reliable as well as simpler in the impact analysis. However, axial load must be applied separately on steel and concrete in order to maintain uniform strain distribution. Which means the numerical simulation process of impact behaviour of columns must contain a contact enforcement verification phase other than the consideration of the mesh discritization.

- Rigid barrier-vehicle impact data are conservative in the impact reconstruction due to the low deformation of the column under shear predominant failure modes. Error induced by the comparatively low stiffness of the concrete column is therefore negligible.

Instead of simulating the impacted vehicle, impact pulse generated from a typical car to rigid barrier impact was successfully used to reconstruct the vehicle collision. This method can be used as the foundation to generate a data base which can be used to determine the vulnerability of column against the impact of new generation of vehicle under all modes of collision.

- Strain rate effects are not predominant under low elevation impact as the shear dominates the failure of the column. On the other hand, it is observed that the average strain rate across the impacted column is less than $0.1s^{-1}$. Therefore, second order strain rate effects can be exempted form the numerical simulation.

- Axially loaded five-story building columns are highly vulnerable to medium velocity car impact. However, at the design stage, impact capacity of the columns can be increased by 20% by selecting the alternative design method with the low steel amount.

- Dynamic interaction force derived based on rigid barrier assumption (EN 1991) is valid only to the shear failure predominate columns and will underestimate the impact capacities of flexure failure predominate columns.

References

[1] http://www.transport.sa.gov.au/safety/road/road_use/roadcrash.asp

[2] Feyerabend, M., Der harte Querstoff auf stutzen aus Stahl und Stahlbeton. University of Karlsruhe (TH), 1988.

[3] El Tawil, S., E. Severino, and P. Fonseca, Vehicle Collision with Bridge Piers. Journal of Bridge Engineering, 2005. 10(3): p. 345-353.

[4] Hallquist, J.O., LS-DYNA 3D: Theoretical manual, Livermore. Livermore Software Technological Corporation, 2006.

[5] Unosson, M., Modelling of concrete material behaviour with application to reinforced concrete beams subjected to impact, SE-147 25, 2001, Swedish defence research agency (FOI), Tumba. p. 33.

[6] Weathersby, J.H., Investigation of bond slip between concrete and steel reinforcement under dynamic loading conditions. 2003, Louisiana State University and Agricultural & Mechanical College: United States-Louisiana.

[7] Bentur, A., S. Mindess, and N. Banthia, The behaviour of concrete under impact loading: Experimental procedures and method of analysis. Materials and Structures, 1986. 19(5): p. 371-378.

[8] Govindjee, S., G.J.K., Juan C. Simo,, Anisotropic modelling and numerical simulation of brittle damage in concrete. International Journal for Numerical Methods in Engineering, 1995. 38(21): p. 3611-3633.

[9] CEB-FIP, CEB-FIP Model Code 1990. Redwood Books, Trowbridge, Wiltshire, UK, 1990.

[10] Flanagan, D.P., Belytschko, T. (1981), "A uniform strain hexahedron and quadrilateral with with orthogonal hourglass control", International Journal for Numerical Methods in Engineering, Vol. 17 pp.679-706.

[11] Varat, M.S. and S.E. Husher, Vehicle impact response analysis through the use of accelerometer data. SAE Technical Paper Series, 2000. SAE World Congress, Detroit, Michigan.

[12] EN 1991-1-7:2006, Eurocode 1 - Actions on structures - Part 1-7: General Actions & Accidental actions. Irish standards, 2006.

[13] http://www-nrd.nhtsa.dot.gov/database/nrd-11/veh_db.html

[14] Breed, D.S., V. Castelli, and W.T. Sanders, A New Automobile Crash Sensor Tester. SAE Technical Paper 910655, 1991. Society of automotive engineers, Warrendale, PA.

[15] AS 1170.1, AS/NZS 1170.1:1989 : Structural design actions, Permanent, imposed and other actions.1989: p. 20.

[16] AS 3600, Concrete structures. 2004: p. 185.

[17] BS 8110, Part 1: structural use of concrete. British Standards Institution, 1985. London. p. 118.

[18] Zielinski, A.J., Concrete structures under impact loading-rate effects, in Department of Civil Engineering. 1984: TH Delft, Delft, Report 5-84-14.

[19] CEB Comite Euro-International du Beton, Concrete structures under impact and impulsive loading. Synthesis Report, 1988. CEB, Lausanne, Switzerland.

[20] Schmidt, M.J. and C.A. Ross, Shear strength of concrete under dynamic loads. American Society of Mechanical Engineers, 1999(Bonton): p. 121-127.

[21] Louw, M.J., G. Maritz, and M.J. Loedolff, The Behaviour of RC Columns under Impact Loading. The Civil Engineer in South Africa, 1992: p. 371-378.